EUROPHYSICS LETTERS 1 September 1989
Europhys. Lett., **10** (1), pp. 25-30 (1989)

Fingering Instabilities of Driven Spreading Films.

S. M. TROIAN (*), E. HERBOLZHEIMER (*), S. A. SAFRAN (*) and J. F. JOANNY (**)
(*) *Exxon Research and Engineering, Annandale, NJ 08801*
(**) *Ecole Normale Superieure, Lyon, France*

(received 8 March 1989; accepted in final form 13 June 1989)

PACS. 47.20 – Hydrodynamic stability and instability.
PACS. 68.45 – Solid-fluid interface processes.

Abstract. – We show that a thin film with small dynamic contact angle and driven by an external body force is unstable to the formation of fingers in the direction perpendicular to the main flow. The instability is largest in the capillary region near the contact line, where the force due to surface tension is comparable to the viscous and gravitational forces. The fastest growing wavelength is calculated in the limit of small-amplitude disturbances. These instabilities may be related to finger patterns observed in gravitational flows and spinning drops.

Recent studies of the physics of dynamic instabilities have focused upon the development of fingers [1] in Hele-Shaw flow. In this paper, we find that a thin wetting film, in an open geometry, driven by an external body force can also be unstable to fingering. The examples considered here are flow of a thin, viscous fluid layer down an inclined plane [2, 3] and the spreading of a rotating drop [4]. In contrast with the Hele-Shaw flows [1, 5], these instabilities occur at the spreading front of a *free surface* profile where there is no pressure gradient in the fluid for the case of uniform flow. Similarly, these fingering instabilities at the front of a viscous film are unrelated to the surface instabilities [6] which arise in systems with nonzero Reynolds numbers. In contrast to the wetting instability discussed here, the wavelength of the surface instability diverges as the Reynolds number vanishes.

The time dependence of the base flow and the finger wavelength of a viscous flow down an inclined plane were studied experimentally by Huppert [2] and by Silvi and Dussan [3]. Huppert suggested a scaling argument to predict the wavelength of the instability and found that this prediction compares favorably with experiment. Recently, Schwartz [7] also studied the fingering phenomenon in gravitational flow within the lubrication approximation and obtained time-dependent, numerical solutions.

We consider the instability of the profile for a liquid film spreading down an inclined plane. The geometry is depicted in fig. 1, where the fluid flows down the plane in the $\hat{x}$ direction, the profile is parameterized by a height H in the $\hat{z}$ direction, and the fingers occur as an instability in the $\hat{y}$ direction. In the presence of both gravity and surface tension, the height profile, $H(x, y)$, is obtained from the solution of the height-averaged continuity

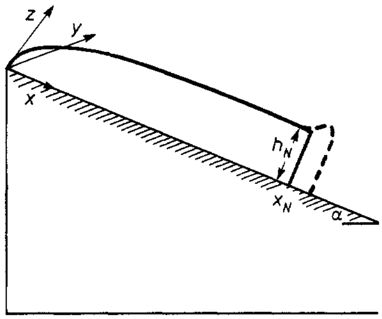

Fig. 1. – Sketch of the profile geometry for flow down an inclined plane. The height in the z-direction has been greatly exaggerated.

equation

$$\frac{\partial H}{\partial t} + \nabla \cdot HV = 0, \tag{1}$$

where t is the time, $V = U\hat{x} + V\hat{y}$, and U and V are the height-averaged velocities in the $\hat{x}$- and $\hat{y}$-directions, respectively. In the lubrication approximation [8], the velocity is

$$\eta V = \frac{H^2}{3}[\rho g \sin\alpha\,\hat{x} + \sigma \nabla \varkappa], \tag{2}$$

where η is the viscosity, ρ is the fluid density, g is the gravitational constant, σ is the surface tension, and α is the angle from the horizontal of the inclined plane. Within our approximations, the curvature, $\varkappa$, is given by $\varkappa \simeq (H_{xx} + H_{yy})$, where $H_x = \partial H/\partial x$.

As in ref. [2], we first consider the unperturbed flow in the region away from the contact line (the outer region), where the capillary pressure (or surface curvature) is negligible and the viscous and gravitational forces balance. The self-similar solution for the one-dimensional flow is [2] $H = (\eta/\rho g \sin\alpha)^{1/2} x^{1/2} t^{-1/2}$. In this approximation, the profile ends abruptly at $x = x_N$, which is determined from volume conservation as $x_N = (9A^2 g \sin\alpha/4\eta)^{1/3} t^{1/3}$, where A is the cross-sectional area of the fluid layer (*i.e.*, the volume of the drop per unit length along $\hat{y}$). At $x = x_N$, the height, H_N, is given by $H_N(t) = 3A/2x_N$.

Naturally, for x near x_N (the inner region), the profile is smoothed by surface tension. This region was discussed by Huppert, who omitted the terms corresponding to the motion of the contact line with the velocity $U_0 = \mathrm{d}x_N/\mathrm{d}t$. Our calculations show that these convective terms are not negligible, even near the contact line. To find the solution for the unperturbed (y-independent) profile in the inner region, we set the contact line as the origin of the coordinate system. The profile is scaled as $H(x, y, t) = H_N(t)\,h(\xi, t)$ so that $h \to 1$ as $\xi \to \infty$ in order to match to the solution ($H \sim h_N$) in the outer region ($x \gg x_N$). The dimensionless length, ξ, is the distance along $\hat{x}$ measured from the contact line and scaled by l which is the characteristic length over which the surface tension competes with the gravity term, $l = H(3Ca)^{-1/3}$, where the capillary number $Ca = \eta U_0/\sigma \ll 1$. In eq. (2), the hydrostatic pressure terms proportional to H_x and H_y are neglected, which is a valid approximation for thin films where the ratio $H_N(t)/l = (3Ca)^{1/3} \ll \operatorname{tg}\alpha$. The scaling indicates that when H_N is used as the characteristic length, the flow in the inner region depends only on the capillary number. With this scaling, a quasi-steady solution of eqs. (1) and (2) determines the function $h(\xi, t) = h_0(\xi)$ when the appropriate boundary conditions are used. For $\xi \to \infty$, the inner and outer solutions must match: all the derivatives, h_x, h_{xx}, ... vanish and $h_0 \to 1$. Near the contact line, the dynamics must take into account the singularities which arise [9] because of the no-slip ($V = 0$ at $H = 0$) boundary condition. Two possible mechanisms which relieve these singularities are i) the presence of a thin film ahead of the contact line [10] or ii) the existence of a region with slip [11].

We choose to match the solution in the inner region to a thin film of thickness bH_N, and the resulting equation for the profile is

$$h_0^2(1 - h_{0_{\xi\xi\xi}}) = \frac{(1-b^3)}{(1-b)} - (1+b)\frac{b}{h}. \tag{3}$$

The solution to eq. (3) is shown in fig. 2, for several values of $b \ll 1$. Within a distance $O(l)$ of the contact line, there is a strong maximum of the profile which decays away to a value of $h_0 \to 1$ in an oscillatory manner as $\xi \to \infty$. The height of the maximum is a weak (logarithmic) function of b.

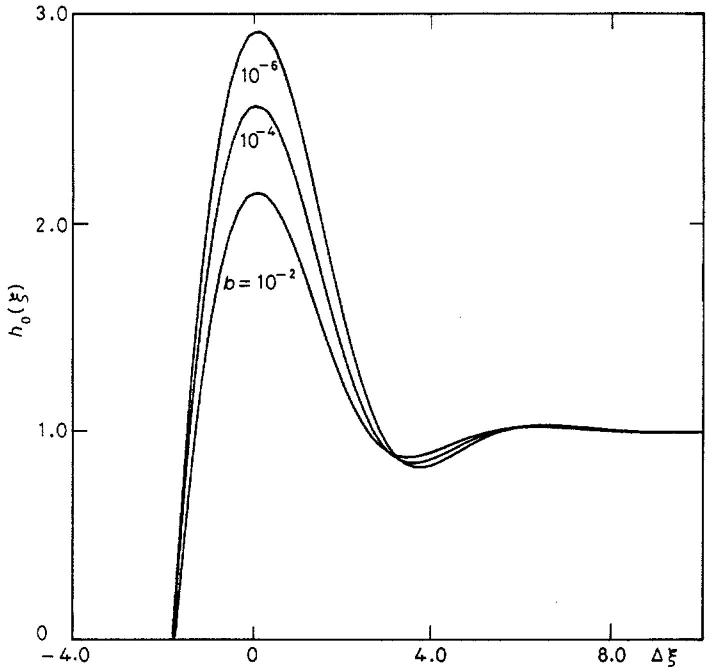

Fig. 2. – Solution of eq. (3) for the unperturbed profile as a function of $\Delta\xi$, which includes an arbitrary shift along the ξ direction so that the maxima line up.

We now consider the linear stability of the uniform profile to small perturbations in the $\hat{y}$ direction. For simplicity, we neglect terms of order $b \ll 1$ in the equations; their inclusion is straightforward. Scaling the y-coordinate by l, we define $\zeta = y/l$, and describe these perturbations by the wave vector Q which corresponds to the dimensionless wave vector $q = Ql$. The position of the boundary is displaced from $\xi = 0$, to a value $\xi = \xi_B$, where

$$\xi_B(\zeta, t) = -A(\zeta)B(t). \tag{4}$$

If $A(\zeta) = \cos q\zeta$, then the region where $-\pi/2 < q\zeta < \pi/2$ represents a section of the boundary perturbed in the forward $\hat{x}$ direction—*i.e.* a finger. The time-dependent amplitude of the perturbation is $B(t)$ and the finger grows if $\partial B/\partial t > 0$. The growth law is calculated from a linear stability analysis, where the scaled film thickness is written as

$$h(\xi, \zeta, t) = h_0(\xi) + A(\zeta)\, h_1(\xi, t), \tag{5}$$

where h_0 is given by eq. (3) and h_1 is the correction to the profile. With these scalings and with the definitions $u = U/U_0$, $v = V/U_0$, one can write to linear order in h_1

$$u = h_0^2[(1 - h_{0_{\xi\xi\xi}})(1 + 2h_0 A h_1) + A h_{1_{\xi\xi\xi}} + A_{\zeta\zeta} h_{1_\xi})], \tag{6}$$

$$v = h_0^2\,[A_\zeta h_{1_{\xi\xi}} + A_{\zeta\zeta\zeta} h_1]. \tag{7}$$

We write $h_1 = G(\xi)\exp[\beta\tau]$ and $B(t) = B_0 \exp[\beta\tau]$ where the effective time variable $\tau = \int U_0(t)/l\,\mathrm{d}t$ is proportional to the distance traveled. The linearized version of the continuity equation then becomes

$$\frac{\partial G}{\partial \tau} + h_0^3[q^4 G - q^2 G_{\xi\xi}] + \frac{\partial}{\partial \xi}[-2G + h_0^3(G_{\xi\xi\xi} - q^2 G_\xi)] = 0. \tag{8}$$

Equation (8) has been derived using a quasi-static approximation so that terms in $(\partial l/\partial t)/U_0 \sim Ca^{2/3}$ have been dropped. Equation (8) must be solved together with the appropriate boundary conditions. For $\xi \to \infty$, we require $h_1 \to 0$, so that h remains unchanged and matches the outer solution. In the region near the contact line, a linearization of the boundary condition $h(\xi_\mathrm{B}, \zeta, t) \to 0$ implies that $h_1(\xi, t) \to B(t)\,\partial h_0/\partial\xi$ as $\xi \to 0$. In principle, more precise boundary conditions are necessary to match the solution to the prewetting film or the slip-region profile; however, as shown below, these conditions for h_1 are unnecessary to find the growth rate of the instability at small q.

To demonstrate that the profile is unstable, we solve eq. (8) in the long-wavelength limit. Noting that only even powers of q appear in the equation, we write $G(\xi) = B_0(g_0 + q^2 g_1(\xi)\ldots)$ and $\beta(q) = \beta_1 q^2 + \ldots$. The zeroth-order equation is

$$[-2g_0 + h_0^3 g_{0_{\xi\xi\xi}}] = 0. \tag{9a}$$

The solution consistent with the boundary conditions is $g_0 = B_0\,\partial h_0/\partial\xi$ which represents a simple translation of the interface. Since $\partial h_0/\partial\xi \to 0$ as $\xi \to \infty$, the translation affects the profile only in the vicinity of the contact line. We note that this is not a proper eigenfunction of a wedge-shaped profile, where $\partial h_0/\partial\xi$ remains finite as $\xi \to \infty$.

The equation to order q^2 is

$$\beta_1 g_0 - h_0^3 g_{0_{\xi\xi}} + \frac{\partial}{\partial\xi}[-2g_1 + h_0^3(g_{1_{\xi\xi\xi}} - g_{0_\xi})] = 0. \tag{9b}$$

Integrating once from $\xi \to \infty$ to $\xi \to 0$ and using the boundary conditions $g_1 \to 0$ as $\xi \to 0$ and $\xi \to \infty$, one finds

$$\beta_1 = \int_0^\infty \mathrm{d}\xi\, h_{0_{\xi\xi\xi}} h_0^3 = \int_0^\infty \mathrm{d}\xi\, h_0(h_0^2 - 1), \tag{10}$$

where the last term in eq. (10) is obtained from eq. (3). Equation (10) is the integral in the $\hat{x}$ direction of the divergence of the flux obtained by displacing the origin of the unperturbed profile, h_0, by $B_0 \cos(q\zeta)$. The integrand in eq. (10) vanishes when $h_0 \to 1$, since the instability arises from the flows in the capillary region only and does not depend on the total length of the system; however, this analysis only holds when $x_N \gg l$. In ref. [7], the initial conditions do not necessarily satisfy this condition, and the profile may be stable until the film has advanced a distance x_N comparable to l, when $H_N \sim A/l$. Using $l = H_N(3Ca)^{-1/3}$ with $H_N \sim A/l$, and resolving for l, one finds that the value of l at which the instability occurs is proportional to $(AL^2)^{1/4}$, with $L^2 = (\sigma/\rho g \sin\alpha)$, in agreement with the results of ref. [7]. We note, however, that this dependence on A is an artifact of the initial conditions. The analysis presented here focuses on the asymptotic profile in the inner region. The predicted finger wavelength depends only on the film thickness and the capillary number and is independent of the cross-sectional area, as is physically reasonable for an instability of the capillary region. Experiments which constrain the film thickness, or which have initial conditions where $H_N/l \ll 1$, should confirm these predictions.

In fig. 3, we present the results [12] of a numerical solution of eq. (8) which has been modified to include the terms of order b which account for the matching to the thin film. The

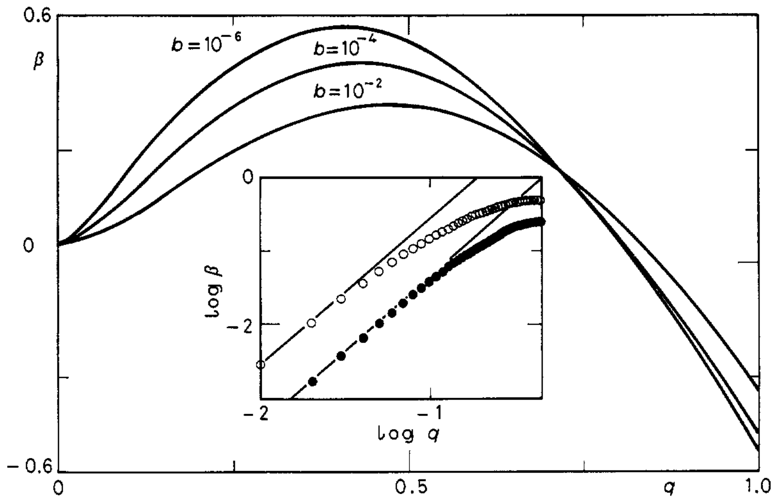

Fig. 3. – Eigenvalue, β, as a function of wavevector, q. Positive values of β indicate unstable modes. The inset shows $\log\beta$ *vs.* $\log q$ for values of $b = 10^{-2}$ (●) and 10^{-6} (○). The solid lines show the prediction of eq. (10).

plot shows the eigenvalue β as a function of the wave vector, q. Also shown is the prediction of eq. (10) (calculated with the numerical solution for h_0 from eq. (3)) which is in good agreement with the numerical results for small values of q. The detailed $\beta(q)$ shows a slow (logarithmic) dependence on b. The profile is unstable for $q \lesssim 0.9$ and the maximum growth rate occurs for $q \approx 0.45$. Thus, the predicted wavelength of the most amplified wave is given by $\lambda = (2\pi/q)\,l \approx 14l$. Huppert fit his experimental data (cf. his eq. (13) with $A = 2H_N x_N/3$) with $\lambda = 7.5l(2x_N/3A^{1/2})^{1/3}$. From his fig. 3, $x_N/A^{1/2}$ appears to be approximately 20 at the onset of the instability which gives $\lambda \approx 18l$. Considering the uncertainty in this procedure for estimating the value of H_N in the experiments, the agreement between theory and experiment is surprisingly good.

One can apply a similar analysis to the situation of a rotating drop with a free surface. In the absence of surface tension, the rotation of a drop of size $R(t)$ with angular velocity ω results in an averaged radial velocity, $\mathrm{d}R/\mathrm{d}t \propto \omega^2 H^2 R$. Using conservation of volume then gives that the height decreases in time as $H_N \sim t^{-1/2}$, where H_N is the film thickness. The radius $R(t) \sim t^{1/4}$ corresponds to $x_N(t)$ in the gravity problem. As before, surface tension smooths the profile near the contact line over a distance l defined in eq. (6), with the result that $l \sim H_N^{1/2}$, if terms of order l/R can be neglected. The calculation of the instability then proceeds as in the gravity case. These same ideas should also apply to other systems where a fluid with a contact line is driven by a body force or a surface shear stress (*e.g.*, air flowing over a liquid layer) and similar instabilities should be observed.

* * *

The authors are grateful to H. HUPPERT, F. MELO, J. STOKES and L. SCHWARTZ for useful discussions.

REFERENCES

[1] For a recent review see BENSIMON R., *Rev. Mod. Phys.*, 58 (1986) 977.
[2] HUPPERT H. E., *Nature (London)*, **300** (1982) 427.
[3] SILVI N. and V. DUSSAN E. B., *Phys. Fluids*, 28 (1985) 5.
[4] TANNER L. H., *La Recherche*, **17** (1986) 184.
[5] JANSONS K. N., *J. Fluids Mech.*, **163** (1986) 59.
[6] YIH C.-S., *Phys. Fluids*, **6** (1963) 321.
[7] SCHWARTZ L. W., *Phys. Fluids A*, **1** (1989) 443.
[8] MOFFAT K., in *Fluid Dynamics*, edited by R. BALIAN and J. L. PEUBE (Gordon and Breach, New York, N. Y.) 1973.
[9] HUH C. and SCRIVEN L. E., *J. Colloid Interface Sci.*, **35** (1971) 85; for reviews see V. DUSSAN E. B., *Ann. Rev. Fluid Mech.*, **11** (1979) 371; DE GENNES P. G., *Rev. Mod. Phys.*, 57 (1985) 827; JOANNY J. F., *J. Theor. Appl. Mech.*, 23 (1986) 249.
[10] DERYAGIN B., *Koloidn. Zh.*, 17 (1955) 191.
[11] HUH C. and MASON S. G., *J. Colloid Interface Sci.*, **60** (1977) 11; HOCKING L. M., *J. Fluid Mech.*, **79** (1977) 209.
[12] HERBOLZHEIMER E., TROIAN S. M. and SAFRAN S. A., to be published.